

Thermal-Barrier Production and Identification in a Tandem Mirror

D. P. Grubb, S. L. Allen, T. A. Casper, J. F. Clauser, F. H. Coensgen, D. L. Correll, W. F. Cummins, C. C. Damm, J. H. Foote, R. K. Goodman, D. N. Hill, E. B. Hooper, Jr., R. S. Hornady, A. L. Hunt, R. G. Kerr, G. W. Leppelmeier, J. Marilleau, J. M. Moller, A. W. Molvik, W. E. Nexsen, W. L. Pickles, G. D. Porter, P. Poulsen, E. H. Silver, T. C. Simonen, B. W. Stallard, and W. C. Turner

Lawrence Livermore National Laboratory, University of California, Livermore, California 94550

and

W. L. Hsu

Sandia National Laboratory, Livermore, California, 94550

and

T. L. Yu

Johns Hopkins University, Baltimore, Maryland 21218

and

J. D. Barter, T. Christensen, G. Dimonte, and T. W. Romesser

TRW Corporation, Redondo Beach, California 90278

and

R. F. Ellis, R. A. James, and C. J. Lasnier

University of Maryland, College Park, Maryland 20742

and

L. V. Berzins, M. R. Carter, C. A. Clower, B. H. Failor, S. Falabella, M. Flammer, and T. Nash

University of California-Davis, Livermore, California 94550

(Received 9 April 1984)

In thermal-barrier experiments in the tandem mirror experiment upgrade, axial confinement times of 50 to 100 ms have been achieved. During enhanced confinement we measured the thermal-barrier potential profile using a neutral-particle-beam probe. The experimental data agree qualitatively and quantitatively with the theory of thermal-barrier formation in a tandem mirror.

PACS numbers: 52.55.Ke

In this Letter we report the first measurements of a thermal barrier in a tandem-mirror plasma device and the resulting enhancement of the axial confinement time.

A thermal barrier in a tandem mirror¹ is a depression in the axial profile of the plasma potential that isolates central-cell electrons from electrons in the ion-confining potential peak [a thermal-barrier potential profile is shown in the west-end-cell region of Fig. 1(b)]. The thermal isolation makes possible selective heating of the electrons in the potential peak, thus enhancing the potential (ϕ_i) that confines central-cell ions. Thermal-barrier theory^{2,3} predicts that it is possible to generate an ion-confining potential even when the central-cell density (n_c) is greater than the end-cell density (n_p). This is a major improvement over a simple tandem mirror,⁴⁻⁶ which requires $n_p > n_c$. It makes possible a reactor with a high central-cell density (for fusion power output) while minimizing the power

and magnetic field required by the end cells.

The axial confinement time in a tandem mirror is long enough that radial transport can be significant.^{7,8} Measurements show radial as well as axial ion losses in the tandem mirror experiment upgrade device (TMX-U). The radial lifetime is in the range of 2 to 100 ms, depending on operating conditions, and appears to be independent of thermal-barrier formation.

The TMX-U device was designed to demonstrate thermal-barrier formation in a tandem mirror. The typical magnetic field configuration⁹ is shown in Fig. 1(a). Each end cell (plug) has six neutral beams (15 kV, 50 A) aimed 47° to the magnetic axis at the plug midplane. These beams fuel the mirror-confined (sloshing) ions¹⁰ and remove trapped ions from the barrier.¹¹ In the central cell, ion-cyclotron resonant heating at 2.48 or 2.64 MHz heats the ions. During these experiments 5 to 40 kW was coupled into the plasma.

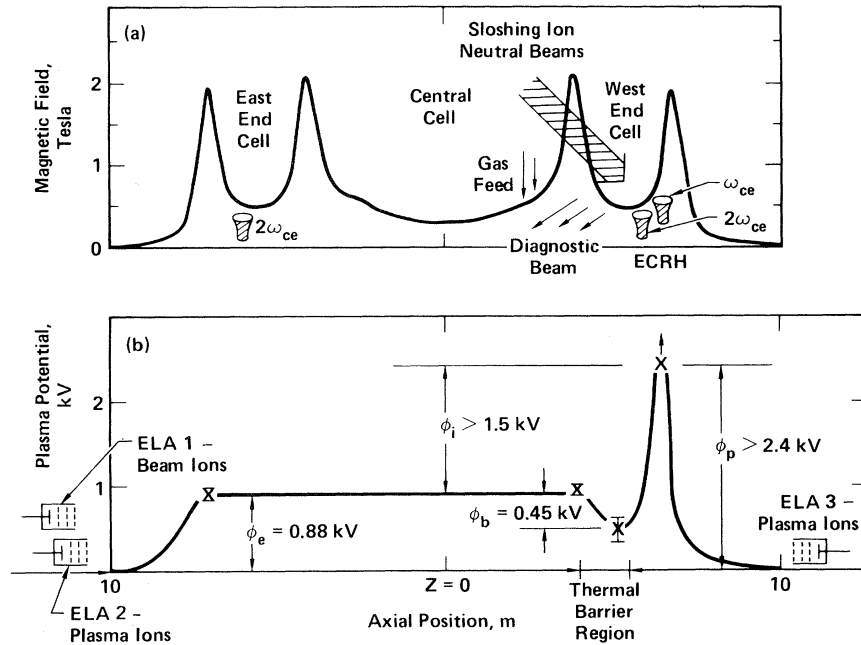


FIG. 1. Axial profiles of (a) magnetic field and (b) expected potential profile during single-end tandem operations including measured potentials (crosses). The measurements do not uniquely define the axial locations of ϕ_e or ϕ_p or the spatial variation of the potential in the barrier region. The theoretical concept (solid line) was used as a model for spatial location of the data. The spatial location of the barrier, however, was uniquely determined by the aiming of the diagnostic beam. The plug potential was set > 2.4 kV because the maximum bias on energy analyzer No. 3 was insufficient to repel any of the plasma ions. This set a lower bound on ϕ_p .

Two pulsed, 28-GHz gyrotron tubes in each plug heat the electrons. The launching structures for the gyrotrons are aimed at the fundamental electron-cyclotron resonance ($B=1$ T) and the second-harmonic resonance ($B=0.5$ T), respectively. For these experiments the maximum pulse length was 50 ms and the heating power varied from 50 to 200 kW per tube.

Figure 2 shows the time history of a thermal-barrier plasma discharge. These discharges begin at low densities to minimize scattering losses of hot electrons and collisional filling of the thermal barrier. Once a thermal barrier is established and enhanced energy confinement is achieved, particle fueling is increased to raise the central-cell density. To date, we have reduced the ion losses with central-cell densities as high as $2 \times 10^{12} \text{ cm}^{-3}$.

Soon after the sloshing-ion beams turn on [Fig. 2(b)], the axial losses [Fig. 2(d)] decrease dramatically (we refer to this as plugging the end losses). Indeed, during strong plugging the ion losses are so small that the dominant current detected by both Faraday cups and ion-energy analyzers¹² on the end walls consists of electrons with energies greater than the 3- to 5-kV electron-repelling grid voltage used in the detectors. (The total energetic-electron

loss current is approximately equal to the classical scattering-loss current of the hot electrons.) Under these conditions, the magnitudes of the ion and energetic-electron currents are determined by the ion-energy analyzers that sweep out the ion-energy spectrum (200-Hz sweep rate) and measure only energetic-electron current when the ion-repeller grid voltage becomes much greater than the average ion energy.

Before plugging, the central-cell-ion axial-confinement time (τ_{\parallel}) is 5 to 10 ms. During plugging we measure

$$\tau_{\parallel} = \frac{\int_0^{14} n(r) 2\pi r dr}{\int_0^{14} j_{\parallel}(r) 2\pi r dr} eL_c = 50 \text{ to } 100 \text{ ms},$$

(at a density of $7 \times 10^{11} \text{ cm}^{-3}$), where $n(r)$ and $j_{\parallel}(r)$ are the radial profiles of plasma density and ion axial-loss current, respectively, $e = 1.6 \times 10^{-19}$ C, and L_c is the effective length of the central-cell plasma (508 cm). The density is measured by microwave interferometry and (for $n \geq 1 \times 10^{12} \text{ cm}^{-3}$) by neutral-beam attenuation. We assume azimuthal symmetry for the integration of the density and current and restrict the integration to the core plasma ($r < 14$ cm) where enhanced axial con-

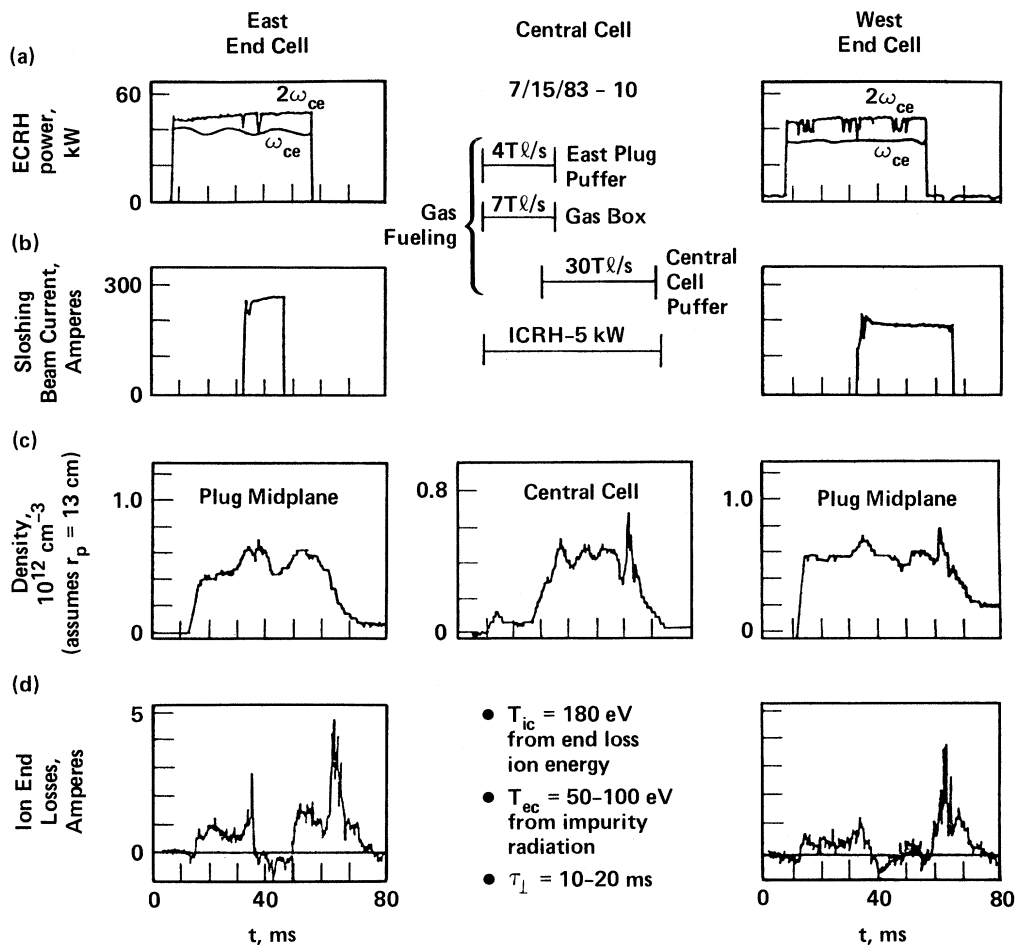


FIG. 2. Time history of TMX-U plasma discharge (double-end operation) showing strong reduction of axial losses during the time that both the sloshing-ion neutral beams and the electron cyclotron resonant heating are on. The central-cell density increase is small because the radial confinement time (τ_{\perp}) is comparable to the unplugged axial lifetime and τ_{\perp} is independent of whether or not the axial losses are plugged.

finement is observed. Outside $r = 14$ cm, enhanced confinement is not expected; at large radii the plug-neutral-beam aiming and the background-gas density limit the sloshing-ion density and increase the barrier filling rate. The plasma limiter is at $r = 26$ cm.

Table I contains a comparison of experimental results with predictions of thermal-barrier theory. The experimental results show that the basic requirements of our thermal-barrier model must be satisfied to generate greatly enhanced axial confinement. In addition, some data indicate that a lesser enhancement of confinement can be achieved without all the thermal-barrier ingredients present. Since these data may point to a simpler way to operate a tandem mirror, further experiments will investigate this phenomenon.

For a limited subset of the plugging data we made direct measurements of the axial potential profile

which show that a thermal-barrier depression is present during plugging and that the magnitude of the potential dip (100 to 600 V) is in the range predicted by theory³ for a central-cell electron temperature (T_{ec}) in the range of 30 to 100 eV.

To make this measurement, we operated TMX-U as a single-end tandem mirror by injecting sloshing-ion neutral beams into the west plug but not the east. The expected axial potential profile during these experiments is shown in Fig. 1(b). We deduced the plug and central-cell potentials from the minimum energy of axially escaping plasma ions. All ions passing through the east plug fell through a potential ϕ_e to reach the energy analyzer. Similarly, the ions passing through the west plug fell through a potential ϕ_p . The ion-energy analyzers located at the end walls of the device measured the energy spectrum of these ions.

A second energy analyzer on the east-end wall

TABLE I. Comparison of theory and experiment.

Theoretical prediction (Refs. 1-3)	Experimental confirmation
Low neutral-gas density required in plugs	Yes ^a
Sloshing-ion beams required for plugging	Yes—Fig. 2
Electron cyclotron resonant heating at potential peak (ω_{ce}) required for plugging	Yes—Fig. 2
Large fraction of hot electrons at barrier required for plugging	Yes—ratio of hot density to total electron density $\geq 80\%$ to establish plugging ^b
Plug electron temperature (T_{ep}) greater than central cell (T_{ec})	$T_{ep} \geq T_{ec}$ ^c
Plugging possible with $n_c > n_p$	Yes—plugging with $n_c/n_p > 1$ to 2

^aRef. 13.^bRef. 14.^cRef. 15.

measured the axial potential variation in the thermal-barrier region of the west plug by measuring the energy spread of neutral-beam-injected ions. A diagnostic neutral beam was injected into the thermal-barrier region of the west plug. The beam did not intercept the axis of the device (where these measurements were made) until 35 cm past the midplane of the plug (these measurements, therefore, place a lower bound on the barrier depth). The beam then passed through the transition magnets into the central cell. Along this path, ions were created by charge exchange and ionization. Since these ions were injected at a shallow angle to the magnetic field (18°), they flowed freely along the field line until they reached the far-end wall where their energy spectrum was measured. The energy spread of these ions is a direct measure of the potential variation along the field line where they were deposited.

The resulting measurement of the axial potential profile is shown in Fig. 1(b). The maximum energy (above the beam-injection energy) in the beam-ion spectrum agrees with the central-cell potential measured by the east plasma-ion analyzer. The lower energy part of the spectrum, therefore, corresponds to a potential depression of 450 V in the region where we expect a thermal barrier to form. Since

this measurement required us to operate TMX-U in a single-end configuration, the number of measurements of the barrier depth is limited and comparisons between ϕ_b and confinement have not yet been attempted.

We have begun to model the TMX-U plugging results reported here with a time-dependent power- and particle-balance code.¹⁶ The initial results show better than a factor of 2 agreement between the experimental measurements and the code predictions.

Finally, the sloshing ions continue to be microstable in TMX-U at densities up to $1 \times 10^{12} \text{ cm}^{-3}$, above which low-level ion-cyclotron fluctuations begin. This result is in agreement with theoretical predictions and is particularly notable because the flow of stabilizing ions is almost totally eliminated during plugging.

In conclusion, results from the initial thermal-barrier experiments in TMX-U show strong reduction in the axial losses with axial confinement times up to 100 ms. The results are consistent with thermal-barrier theory and measurements confirm the formation of a thermal barrier in TMX-U.

The authors gratefully acknowledge the input and support provided by the theory, computations, engineering, and technical groups with the TMX-U experiment. This work was performed under the auspices of the U. S. Department of Energy by the Lawrence Livermore National Laboratory under Contract No. W-7405-ENG-48.

¹D. E. Baldwin and B. G. Logan, Phys. Rev. Lett. **43**, 1318 (1979).

²R. H. Cohen, *et al.*, Nucl. Fusion **20**, 1421 (1980).

³R. H. Cohen, Phys. Fluids **26**, 1977 (1983); Y. Matsuda and T. D. Rognlien, Phys. Fluids **26**, 1778 (1983).

⁴D. L. Correll *et al.*, Nucl. Fusion **22**, 223 (1982).

⁵K. Yatsu *et al.*, Phys. Rev. Lett. **43**, 627 (1979).

⁶R. Breun *et al.*, Phys. Rev. Lett. **47**, 1833 (1981).

⁷A. A. Mirin *et al.*, Nucl. Fusion **23**, 703 (1983).

⁸R. P. Drake *et al.*, Phys. Fluids **25**, 2110 (1982).

⁹J. H. Foote *et al.*, J. Fusion Energy **2**, 383 (1982).

¹⁰T. C. Simonen *et al.*, Phys. Rev. Lett. **50**, 1668 (1983).

¹¹A. H. Futch and L. L. Lodestro, Lawrence Livermore National Laboratory Report No. UCRL-87249, 1982 (unpublished).

¹²A. W. Molvik, Rev. Sci. Instrum. **52**, 704 (1981).

¹³W. C. Turner *et al.*, to be published.

¹⁴W. C. Turner *et al.*, in Proceedings of the 1984 International Conference on Plasma Physics, Lausanne, Switzerland, June 27–July 3, 1984 (to be published).

¹⁵R. K. Goodman and T. D. Rognlien, Lawrence Livermore National Laboratory Report No. UCID-19943, 1982 (unpublished).

¹⁶M. E. Rensink, Bull. Am. Phys. Soc. **28**, 1036 (1983).